Available online at www.sciencedirect.com
ScienceDirect
Journal of Solid State Chemistry 180 (2007) 2740–2746
JOURNAL OF SOLID STATE CHEMISTRY
www.elsevier.com/locate/jssc

$La_3Ru_8B_6$ and $Y_3Os_8B_6$, new members of a homologous series $R(A)_nM_{3n-1}B_{2n}$

O.L. Sologub[a,*,1], L.P. Salamakha[a,d], H. Noël[b], T. Roisnel[c], A.P. Gonçalves[a]

[a]*Departamento de Química, Instituto Tecnológico e Nuclear/CFMC-UL, Estrada Nacional 10, P-2686-953 Sacavém Codex, Portugal*
[b]*Laboratoire de Chimie du Solide et Materiaux, UMR CNRS 6226, Université de Rennes 1, France*
[c]*Centre de Diffractométrie X, UMR 6226, CNRS-Université de Rennes 1, France*
[d]*Department of Physics of Metals, Faculty of Physics, L'viv National University, Kyryla i Mefodiya str. 8, 79005 L'viv, Ukraine*

Received 20 December 2006; received in revised form 21 February 2007; accepted 26 February 2007
Available online 7 March 2007

Abstract

Two new compounds, $La_3Ru_8B_6$ and $Y_3Os_8B_6$, were synthesized by arc melting the elements. Their structural characterization was carried out at room temperature on as-cast samples by using X-ray diffractometry. According to X-ray single-crystal diffraction results these borides crystallize in *Fmmm* space group (no. 69), $Z = 4$, $a = 5.5607(1)$ Å, $b = 9.8035(3)$ Å, $c = 17.5524(4)$ Å, $\rho = 8.956\,Mg/m^3$, $\mu = 25.23\,mm^{-1}$ for $La_3Ru_8B_6$ and $a = 5.4792(2)$ Å, $b = 9.5139(4)$ Å, $c = 17.6972(8)$ Å, $\rho = 13.343\,Mg/m^3$, $\mu = 128.23\,mm^{-1}$ for $Y_3Os_8B_6$. The crystal structure of $La_3Ru_8B_6$ was confirmed from Rietveld refinement of X-ray powder diffraction data. Both $La_3Ru_8B_6$ and $Y_3Os_8B_6$ compounds are isotypic with the $Ca_3Rh_8B_6$ compound and their structures are built up from $CeCo_3B_2$-type and $CeAl_2Ga_2$-type structural fragments taken in ratio 2:1. They are the members of structural series $R(A)_nM_{3n-1}B_{2n}$ with $n = 3$ (R is the rare earth metal, A the alkaline earth metal, and M the transition metal). Structural and atomic parameters were also obtained for $La_{0.94}Ru_3B_2$ compound from Rietveld refinement ($CeCo_3B_2$-type structure, *P6/mmm* space group (no. 191), $a = 5.5835(9)$ Å, $c = 3.0278(6)$ Å).

Keywords: Rare earth intermetallic compounds; X-ray single-crystal diffraction; X-ray powder diffraction; Crystal structure of $La_3Ru_8B_6$ and $Y_3Os_8B_6$; Rietveld refinement of $La_{0.94}Ru_3B_2$

1. Introduction

In the course of our work on structural and magnetic characterization of new intermetallics with potentially promising physical properties, our attention was drawn by Y–Os–B [1,2] system. The formation of five yttrium osmium borides was previously reported in the literature: $YOsB_2$ [3], YOs_4B_4 [1], $YOsB_4$ [4], YOs_3B_2 [5] and Y_2OsB_6 [6]. From magnetic and electrical transport measurements, the YOs_3B_2 sample was observed to display superconducting properties at 5.5 K [7].

The crystal structure of YOs_3B_2 was not completely determined. However, for the so-called "YOs_3B_2" type, an orthorhombic deformation variant of $CeCo_3B_2$ type [5] was suggested, which itself is a derivative structure of $CaCu_5$ type. Isotypic $LaRu_{3-x}B_2$ ($x = 0.25$) compound was claimed to form in La–Ru–B system [5]. Bearing on previous numerous reports on variety of $CaCu_5$-type-related structures of borides (e.g., $CeCo_3B_2$, *P6/mmm*, $a = 5.057$ Å, $c = 3.036$ Å [8]; $ErIr_3B_2$, *C2/m*, $a = 5.409$ Å, $b = 9.379$ Å, $c = 3.101$ Å, $\beta = 91.2^\circ$ [9]; $CeCo_4B$, *P6/mmm*, $a = 5.005$ Å, $c = 6.932$ Å [2]; $NdNi_4B$, *Imma*, $a = 5.057$ Å, $b = 6.980$ Å, $c = 26.271$ Å [10]; $Y_{0.915}Ni_{4.12}B$, *P6/mmm*, $a = 14.908$, $c = 6.919$ Å [11]; $Ce_2Co_7B_3$, *P6/mmm*, $a = 5.053$ Å, $c = 12.97$ Å [12]; $Ce_3Co_{11}B_4$, *P6/mmm*, $a = 5.045$ Å, $c = 9.925$ Å [12]; $Nd_3Ni_{13}B_2$, *P6/mmm*, $a = 5.005$ Å, $c = 10.904$ Å [13]; $Lu_5Ni_{19}B_6$, *P6/mmm*, $a = 4.943$ Å, $c = 17.161$ Å [14]), we decided to perform more detailed structural studies for the samples of composition close to $LaRu_3B_2$ and YOs_3B_2. Several alloys were synthesized within the 16.66 at% La (*Y*) isoconcentrate slightly varying the content of Ru(Os) and B.

*Corresponding author. Fax: +351 21 994 61 85.
E-mail address: sologub@itn.pt (O.L. Sologub).
[1]On leave from Research Center of Low Temperature Studies, L'viv National University, L'viv, Ukraine.

0022-4596/$ - see front matter © 2007 Elsevier Inc. All rights reserved.
doi:10.1016/j.jssc.2007.02.019

All obtained samples were found to be multiphase. Analysis of X-ray powder diffraction patterns revealed the presence of unknown isotypic phases structurally related to $CeCo_3B_2$ type. The results of X-ray single-crystal investigations for these compounds, as well as Rietveld refinement for $La_{16.6}Ru_{50}B_{33.4}$ sample, are given in this paper.

2. Experimental

Samples with a total weight of 0.5 g each were synthesized by arc melting the proper amounts of the constituent elements under high-purity argon on a water-cooled copper hearth. The ingots of lanthanum and yttrium (Alfa Aesar Johnson Matthey Gmbh., 99.9%), boron (Aldrich Chem. Co., 99.7%), and re-melted pellets of compacted ruthenium and osmium powder (Alfa Aesar Johnson Matthey Gmbh., 99.95%) were used as starting materials.

Intensity X-ray diffraction data from single crystals were collected with a Nonius Kappa CCD diffractometer. The complete strategy to fill more than a hemisphere was automatically calculated with the use of the program COLLECT [15].

Philips X'Pert diffractometer (Cu$K\alpha$ radiation, 2θ range 20–115°, step width of 0.02°, a constant counting time of 30 s per step) was used to collect X-ray powder diffraction data. Automatic indexing and lattice parameters refinement were accomplished using the WinPlotr [16], TREOR [17], DICVOL [18] and Powder Cell [19] programs. Structure refinements from powder X-ray diffraction data were performed with the assistance of FullProf program [20].

3. Results and discussion

3.1. Single-crystal X-ray diffraction

Several crystals were selected from as-cast $La_{16.6}Ru_{50}B_{32.4}$ and $Y_{16.6}Os_{50}B_{32.4}$ samples and tested with Nonius Kappa CCD diffractometer (Mo$K\alpha$ radiation, $\lambda = 0.71073$ Å, ω-scan). The crystal of better quality of each alloy was measured. The face-centered orthorhombic unit cells were determined from first 10 measured frames of each single-crystal diffraction data. 448 and 350 images, with total exposure times of 11.0 and 11.3 h, respectively were collected for lanthanum ruthenium boride and yttrium osmium boride crystals, respectively. After integration of all the collected frames with the EVAL program [21] of the Kappa CCD software package, data merging process has been performed using the SADABS program [22]. Further experimental details are listed in Table 1.

For space group determination, crystal structure solution and refinement, the program package WinGX 1.70 [23] was used. The space group extinctions for both crystals lead to the possible *Fmmm* (no. 69), *Fmm2* (no. 42) and *F222* (no. 22) space groups [24], from which *Fmmm* was found to be correct during the refinements. The structures were solved with the aid of SHELXS-97 [25] using a Patterson function, which resulted in the positions of the La(Y) and Ru(Os) atoms. The positions of boron atoms were localized from difference Fourier synthesis. The structures were refined by a full-matrix least-square program package SHELXL-97 [26]. No deviations from full occupation of atomic positions were observed in result of refinement of occupancies. The formulae derived from the structure refinement led to $La_3Ru_8B_6$ ($Y_3Os_8B_6$). Tables 2 and 3 present the standardized coordinates (STIDY [27]) and thermal parameters for all atoms for $La_3Ru_8B_6$ and $Y_3Os_8B_6$, respectively. Selected interatomic distances are given in Tables 4 and 5. Further details of the crystal structure investigations can be obtained from the

Table 1
Parameters for the single-crystal X-ray data collection and refinement for the $Y_3Os_8B_6$ and $La_3Ru_8B_6$ compounds

Crystal	$La_3Ru_8B_6$	$Y_3Os_8B_6$
Lattice parameters (Å)		
A	5.5607(1)	5.4792(2)
B	9.8035(3)	9.5139(4)
C	17.5524(4)	17.6972(8)
Cell volume (Å^3)	956.86(4)	922.53(7)
Space group	*Fmmm* (no. 69)	
Formula per unit cell	4	
Calculated density (Mg/m^3)	8.956	13.343
Absorption coefficient (mm^{-1})	25.23	128.23
Data collection	Nonius Kappa CCD diffractometer	
Theta range for data collection (deg)	4.16–42.00	4.28–27.41
Data set	$-10 \leqslant h \leqslant 9$ $-13 \leqslant k \leqslant 18$ $-32 \leqslant l \leqslant 29$	$-7 \leqslant h \leqslant 7$ $-11 \leqslant k \leqslant 12$ $-18 \leqslant l \leqslant 22$
Number of measured reflections	5611	2341
Number of unique reflections ($R_{int} = 0.0417$)	951 ($R_{int} = 0.0272$)	312
Number of reflections with $I > 2\sigma(I_0)$	776	275
Number of refined parameters	26	
R_1, wR_2 ($I > 2\sigma(I_0)$)	0.0251, 0.0516	0.0377, 0.0971
R_1, wR_2 (all data)	0.0384, 0.0540	0.0444, 0.1005
Goodness of fit on F^2	1.148	1.284
Extinction coefficient	0.00038(3)	0.00011(2)
Largest diff. peak and hole (e/Å^3)	4.506/−2.544	2.894/−6.862
Refinement method	Full-matrix least squares on F^2	

Table 2
Atomic coordinates and thermal parameters for $La_3Ru_8B_6$ obtained from single-crystal X-ray diffraction

Atom	Wyckoff position	x	y	z	$U_{eq.} \times 10^2$(Å^2)
La1	8(i)	0	0	0.18181(2)	0.879(8)
La2	4(a)	0	0	0	1.001(9)
Ru1	16(j)	$\frac{1}{4}$	$\frac{1}{4}$	0.08590(2)	0.478(6)
Ru2	8(i)	0	0	0.41370(2)	0.675(8)
Ru3	8(f)	$\frac{1}{4}$	$\frac{1}{4}$	$\frac{1}{4}$	0.412(8)
B1	16(m)	0	0.16344(47)	0.32848(23)	0.702(63)
B2	8(h)	0	0.33122(68)	0	0.760(91)

Table 3
Atomic coordinates and thermal parameters for $Y_3Os_8B_6$

Atom	Wyckoff position	x	y	z	$U_{eq.}$[a] $\times 10^2$(Å^2)
Y1	8(i)	0	0	0.17916(18)	0.53(7)
Y2	4(a)	0	0	0	0.65(9)
Os1	16(j)	$\frac{1}{4}$	$\frac{1}{4}$	0.08994 (5)	0.29(4)
Os2	8(i)	0	0	0.41955(7)	0.27(4)
Os3	8(f)	$\frac{1}{4}$	$\frac{1}{4}$	$\frac{1}{4}$	0.22(4)
B1	16(m)	0	0.1479(23)	0.3225(14)	0.45(44)
B2	8(h)	0	0.31926 (30)	0	0.01(53)

[a] $U_{iso.}$ for B atoms.

Table 4
Interatomic distances (d, Å) and coordination numbers of atoms (CN) in $La_3Ru_8B_6$ ($d_{max\ La-La} = 4.26$ Å, $d_{max\ La-Ru} = 3.77$ Å, $d_{max\ La-B} = 3.26$ Å, $d_{max\ Ru-Ru} = 3.28$ Å, $d_{max\ Ru-B} = 2.77$ Å, $d_{max\ B-B} = 2.26$ Å)

Atom	d	CN	Atom	d	CN
La1–2B1	3.032(4)	19	Ru3–4B1	2.134(3)	12
La1–4Ru3	3.0614(2)		Ru3–2Ru3	2.7804(1)	
La1–La2	3.1912(4)		Ru3–2Ru1	2.8804(4)	
La1–4B1	3.214(2)		Ru3–4La1	3.0614(2)	
La1–2Ru2	3.2467(3)				
La1–4Ru1	3.2823(3)				
La1–2La1	3.6689(3)				
La2–4Ru2	3.1662(2)	20	B1–2Ru3	2.134(3)	8
La2–2La1	3.1912(4)		B1–1Ru2	2.192(4)	
La2–8Ru1	3.1957(2)		B1–2Ru1	2.216(3)	
La2–4B2	3.236(4)		B1–1La1	3.032(4)	
La2–2B2	3.247(7)		B1–2La1	3.214(2)	
Ru1–2B2	2.200(2)	14	B2–4Ru1	2.200(2)	9
Ru1–2B1	2.216(3)		B2–2Ru2	2.243(5)	
Ru1–2Ru1	2.7804(1)		B2–2La2	3.236(4)	
Ru1–2Ru2	2.8177(1)		B2–1La2	3.247(7)	
Ru1—Ru3	2.8804(4)				
Ru1—Ru1	3.0155(5)				
Ru1–2La2	3.1957(2)				
Ru1–2La1	3.2823(3)				
Ru2–2B1	2.192(4)	13			
Ru2–2B2	2.243(5)				
Ru2–4Ru1	2.8177(1)				
Ru2–1Ru2	3.0295(5)				
Ru2–2La2	3.1662(2)				
Ru2–2La1	3.2467(3)				

Fachinformationszentrum Karlsruhe, 76344 Eggenstein-Leopoldshafen, Germany (fax: (49) 7247-808-666, e-mail: crysdata@fiz.karlsruhe.de) on quoting the depository numbers 417472 and 417473.

3.2. X-ray powder diffraction

Both $La_{16.6}Ru_{50}B_{33.4}$ and $Y_{16.6}Os_{50}B_{33.4}$ alloys were found to be multiphasic from X-ray powder diffraction data analysis. Lanthanum ruthenium boride sample appeared to contain two phases, i.e. $La_3Ru_8B_6$ (78%) and a compound isotypic with $CeCo_3B_2$ type (22%). For multiphase Rietveld refinement of this sample, the experimentally determined $K_{\alpha 2}/K_{\alpha 1}$ ratio of 0.5, $\cos\theta = 0.7998$ for the monochromator polarization correction and a pseudo-Voigt profile shape function were used. The background was refined with a polynomial function. Initial positional parameters for $La_3Ru_8B_6$ were taken from single-crystal refinement, and for ~$LaRu_3B_2$—those characteristic for $CeCo_3B_2$ type of structure were used [8]. The angular dependence of the peak full-width at half-maximum (FWHM) was described by Caglioti's formula [28]. Initial unit cell parameters were obtained with the assistance of PowderCell Program [19]. Parameters obtained from Rietveld refinements of $La_{16.6}Ru_{50}B_{33.4}$ powder diffraction data are given in Table 6, together with refined atomic coordinates and thermal parameters for both phases. Observed, calculated and difference profiles for the $La_{16.6}Ru_{50}B_{32.4}$ sample are shown in Fig. 1.

Table 5
Interatomic distances (d, Å) and coordination numbers of atoms (CN) in $Y_3Os_8B_6$ ($d_{max\ Y-Y} = 4.06$ Å, $d_{max\ Y-Os} = 3.62$ Å, $d_{max\ Y-B} = 3.24$ Å, $d_{max\ Os-Os} = 3.19$ Å, $d_{max\ Os-B} = 2.72$ Å, $d_{max\ B-B} = 2.26$ Å)

Atom	d	CN	Atom	D	CN
Y1–2B1	2.91(2)	19	Os3–4B1	2.11(2)	12
Y1–4Os3	3.017(1)		Os3–2Os3	2.7391(11)	
Y1–4B1	3.08(1)		Os3–2Os1	2.8325(9)	
Y1–4Os1	3.166(2)		Os3–4Y1	3.017(1)	
Y1—Y2	3.171(3)				
Y1–2Os2	3.249(2)				
Y1–2Y1	3.714(3)				
Y2–2B2	3.04(3)	20	B1–2Os3	2.11(2)	8
Y2–4Os2	3.087(1)		B1–1Os2	2.21(2)	
Y2–2Y1	3.171(3)		B1–2Os1	2.27(2)	
Y2–8Os1	3.172(1)		B1–1Y1	2.91(2)	
Y2–4B2	3.24(2)		B1–2Y1	3.08(1)	
Os1–2B2	2.20(1)	14	B2–4Os1	2.20(1)	9
Os1–2B1	2.27(2)		B2–2Os2	2.23(2)	
Os1–2Os1	2.7396(1)		B2–1Y2	3.04(3)	
Os1–2Os2	2.7499(1)		B2–2Y2	3.14(1)	
Os1—Os3	2.8325(9)				
Os1–2Y1	3.166(2)				
Os1–2Y2	3.172(1)				
Os1—Os1	3.183(1)				
Os2–2B1	2.21(2)	13			
Os2–2B2	2.23(2)				
Os2–4Os1	2.7499(1)				
Os2–1Os2	2.847(2)				
Os2–2Y2	3.087(1)				
Os2–2Y1	3.249(2)				

Strong reflections of $Y_{16.6}Os_{50}B_{32.4}$ powder diffraction pattern were indexed on the basis of a face-centered orthorhombic unit cells leading to unit cell parameters $a = 5.4682$ Å, $b = 9.5260$ Å, $c = 17.6868$ Å. The intensities resembled a good agreement with those calculated on the basis of atomic models determined from $La_3Ru_8B_6$ and $Y_3Os_8B_6$ single crystals; however, a significant amount of unknown phase prevent the successful accomplishment of structural refinement from powder data for this alloy.

Table 6
Parameters of structural refinements from X-ray powder diffraction data for the $La_{16.6}Ru_{50}B_{33.4}$ sample; atomic coordinates and thermal parameters of observed compounds

Compound	$La_3Ru_8B_6$		$La_{0.94}Ru_3B_2$
Space group	*Fmmm* (no. 69)		*P6/mmm* (no. 191)
Cell parameters (Å)	$a = 5.5572(5)$ $b = 9.7930(9)$ $c = 17.5523(17)$		$a = 5.5831(9)$ $c = 3.0272(5)$
Volume (Å^3)	955.2(1)		81.72(2)
Number of reflections	225		40
Zero-point (2θ deg)		−0.041(5)	
η (pseudo-Voigt)		0.81(5)	
Half-width parameters			
U		0.25(2)	
V		−0.19(2)	
W		0.063(5)	
Reliability factors, (%)			
R_f	7.36		5.51
R_B	14.0		7.83
Atomic coordinates and thermal parameters (B, Å^2)	La1: 8(i), $z = 0.1850(2)$, $B = 0.65(1)$		La: 1(a), $B = 0.49(2)$[a]
	La2: 4(a), $B = 0.59(2)$		Ru: 3(g), $B = 0.46(2)$
	Ru1:16(j), $z = 0.0853(2)$, $B = 0.60(1)$		B: 2(c), $B = 0.6$[b]
	Ru2:8(i), $z = 0.4204(4)$, $B = 0.59(1)$		
	Ru3:8(f), $B = 0.55(2)$		
	B1:16(m), $y = 0.21(1)$,$z = 0.329(6)$, $B = 0.9$[b]		
	B2:8(h), $y = 0.30(1)$, $B = 0.9$[b]		

[a]Occupancy parameter was refined to be 0.94.
[b]Fixed parameter.

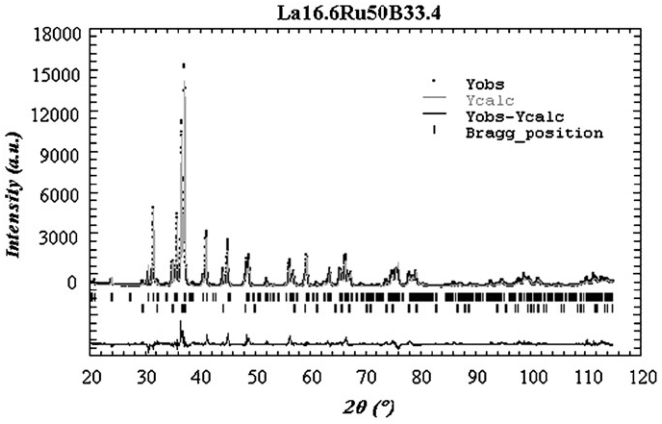

Fig. 1. Experimental (solid black line), calculated (gray crosses), Bragg positions (black vertical bars) and differential (solid black line) powder diffraction profiles for $La_{16.6}Ru_{50}B_{33.4}$ sample.

3.3. Crystal structure description

Projections of the $La_3Ru_8B_6$ structure on *XY* and *XZ* planes and coordination polyhedra for atoms are presented in Fig. 2.

The structure of $La_3Ru_8B_6$ has two crystallographically different atomic positions of La, both with high coordination numbers, as is typical for rare earth atom in intermetallic compounds. The coordination number (CN) of La2 (Fig. 2b) is the same as for Ce in $CeCo_3B_2$ (CN = 20) (Fig. 3a) [8] and its coordination polyhedron (CP) differs from that of Ce by a slight deformation of faces. The La2–La1 contact distance is shorter than the sum of covalent radii of two La atoms ($d_{La2-La1} = 3.1912(4)$ Å). However, these shortened contacts are typical for rare earth atoms in $CeCo_3B_2$-type compounds ($d_{Ce-Ce} = 3.036$ Å for $CeCo_3B_2$, $d_{Y-Y} = 3.038$ Å for YCo_3B_2 [8]), as well as in the structures containing $CeCo_3B_2$ structural fragments [29]. CP for La1 atom has 19 atoms (Fig. 2a) and its shape comprises a combination of one-half of rare earth atom polyhedron in $CeCo_3B_2$-type structure compounds and one-half of a polyhedron of La (Fig. 4a) in $LaCo_2B_2$ [30] ($CeAl_2Ga_2$-type structure [31]).

The coordination sphere of Ru1 (Fig. 2c) is similar to that of Co in $CeCo_3B_2$ (Fig. 3b) and corresponds to a deformed cubooctahedron with two additional atoms of ruthenium placed against the faces which are formed by two lanthanum and two boron atoms. The CN of Ru2 is 13 and its polyhedron differs from that of Ru1 by the absence of one ruthenium atom (Fig. 2d). The CP for Ru3 is 12-apexes distorted cubooctahedron which is slightly deformed as compare to CP of Co in $LaCo_2B_2$ (Figs. 2e and 4b , respectively).

The first coordination sphere of B2 is trigonal prism built by six ruthenium atoms with three additional atoms of lanthanum located against rectangular faces (Fig. 2g) and is similar to that of B atom in the structure of $CeCo_3B_2$ (Fig. 3c). The CP of B1 has a shape of deformed tetragonal antiprism (Fig. 2f) and differs from CP of boron atom in $LaCo_2B_2$ by the shape of larger face which is formed in presented structure by atoms of different type (three lanthanum and one ruthenium). In intermetallic compounds, the Archimedean cube atomic coordination sphere usually possesses one additional atom against larger face [32]. However, in $La_3Ru_8B_6$ and $Y_3Os_8B_6$ as well as in $LaCo_2B_2$ and other rare earth ternary borides of $CeAl_2Ga_2$-type structure, the neighboring B1(B) atom is located too far from the B1(B) central atom to be included in its coordination sphere ($d_{B1-B1} = 3.204(2)$ Å for $La_3Ru_8B_6$, $d_{B1-B1} = 2.814(2)$ Å for $Y_3Os_8B_6$, and $d_{B-B} = 2.48$ Å for $LaCo_2B_2$) and consequently the formation of B–B pairs is rather relative.

3.4. Structural relationships

The characteristic environments of the La(Y), Ru(Os) and B atoms suggest a structural similarity of investigated structure with $CeCo_3B_2$ type and $CeAl_2Ga_2$

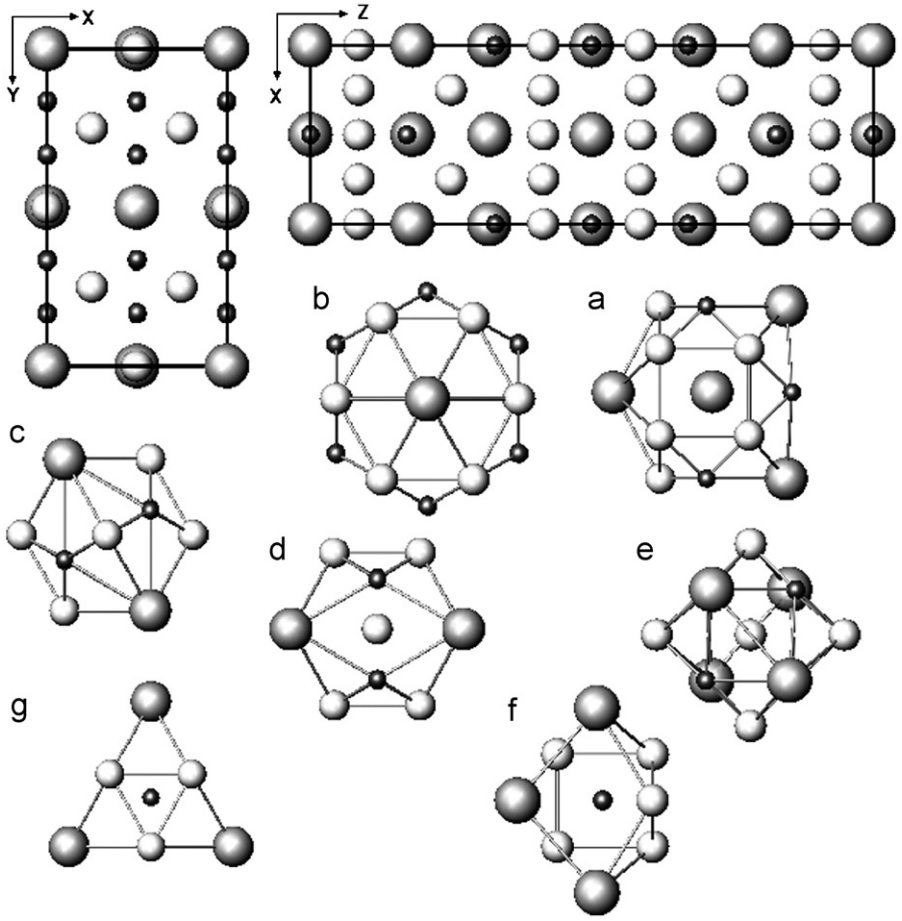

Fig. 2. Projections of $La_3Ru_8B_6$ unit cell on *XY* and *XZ* planes and coordination polyhedra of atoms: La1—a, La2—b, Ru1—c, Ru2—d, Ru3—e, B1—f, B2—g. Large dark gray circles stand for La atoms, smaller light gray circles—for Ru atoms, and small black circles—for B atoms.

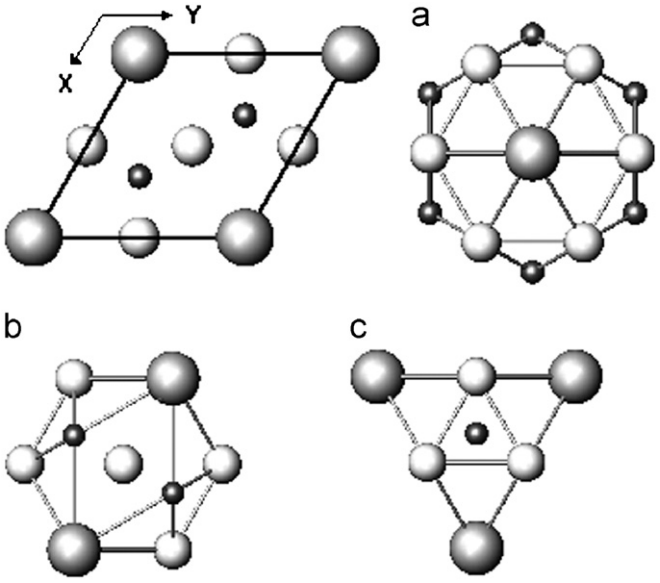

Fig. 3. Projections of $CeCo_3B_2$ unit cell on *XY* plane and coordination polyhedra of atoms Ce—a, Co—b, B—c. Ce atoms are drawn as large dark gray circles, Co atoms are smaller light gray circles, and B atoms—small black circles.

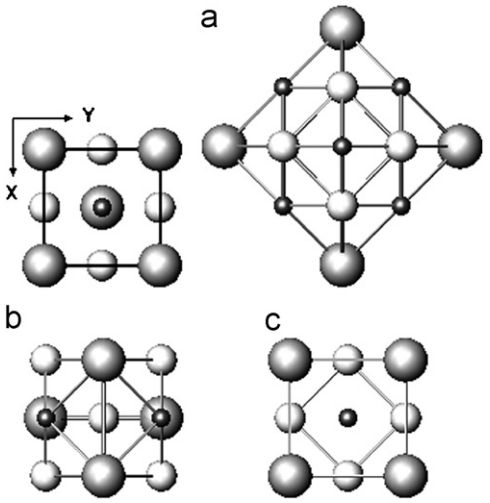

Fig. 4. Projections of $LaCo_2B_2$ unit cell on *XY* plane and coordination polyhedra of atoms La—a, Co—b, B—c. La atoms are presented as large dark gray circles, Co atoms are smaller light gray circles, and B atoms are small black circles.

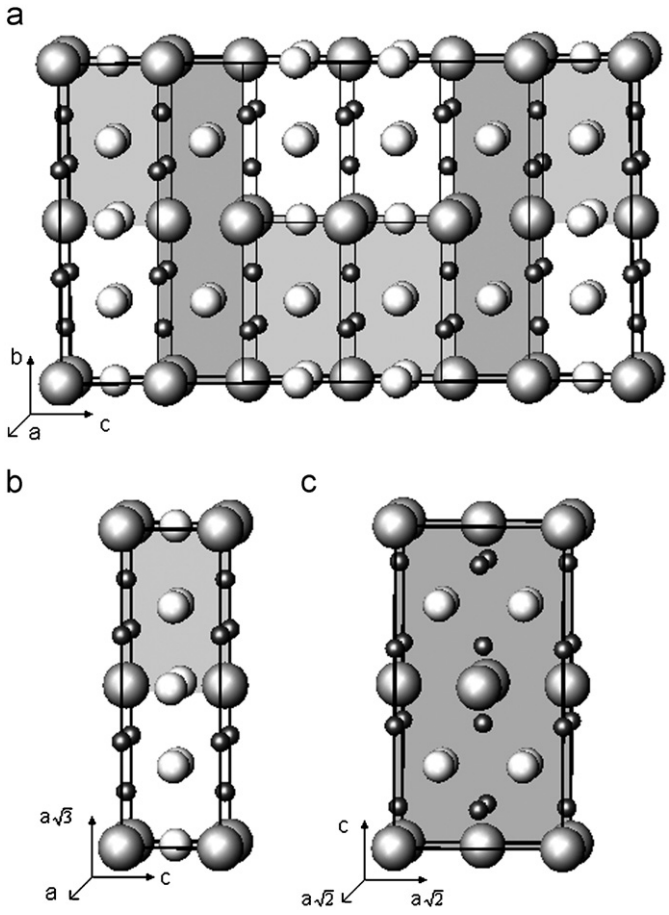

Fig. 5. $La_3Ru_8B_6$ unit cell (a) as arrangement of $CeCo_3B_2$-type (b) and $CeGa_2Al_2$-type structural fragments (c). Large dark gray circles stand for rare earth metal atoms, smaller light gray circles—for the atoms of transition metal, small black circles stand for B atoms.

type. Comparison of all three structures shows that effectively the structure of $La_3Ru_8B_6$ ($Y_3Os_8B_6$) represents the intergrowth of $CeCo_3B_2$-type and $CeAl_2Ga_2$-type structural fragments taken in ratio 2:1 (Fig. 5). Consequently, the structure contains typical for $CeCo_3B_2$ layers of B2 trigonal prisms connected by vertical edges to form a hexahedral rings where the rare earth atoms are located (one R atom per ring in $La_3Ru_8B_6$ and $Y_3Os_8B_6$ structures) (Fig. 6a). These sheets are stretched in XY plane and alternate in the z direction with the zig-zag like walls composed of two columns built up of tetragonal antiprisms of B1 stacked in inverse way via rectangular faces (Fig. 6b).

Both compounds belong to the $Ca_3Rh_8B_6$ structural family and are new members of a homologues series $R(A)_nM_{3n-1}B_{2n}$ with $n=3$ ($n=2$: $Ca_2Rh_5B_4$ and $Sr_2Rh_5B_4$, $n=5$: $Sr_5Rh_{14}B_{10}$, $n=7$: $Ca_7Rh_{20}B_{14}$ [33]). The relationships between $Ca_3Rh_8B_6$-, $CeCo_3B_2$- and $CaRh_2B_2$-type [34] (Fig. 7) structures were described earlier by Jung [33]. $CaRh_2B_2$ structure itself (*Fddd* space group (no. 70), $a=5.832$ Å, $b=9.240$ Å, $c=10.606$ Å) and its derivative $CeRu_2B_2$ (*F222* space group (no.22), $a=6.4861$ Å, $b=9.0573$ Å, $c=10.0263$ Å) [35] are the stacking variants of $CeAl_2Ga_2$ type.

Similarly to $CeCo_3B_2$, the $Ca_3Rh_8B_6$ (Figs. 8a and b) and $CaRh_2B_2$ (Figs. 8c and d) structures contain Ca,B-layers and Rh-layers. In $CaRh_2B_2$, $\frac{1}{3}$ of atoms per each Rh-layer is missing, as compare to $CeCo_3B_2$, and the layers are shifted for $\frac{1}{2}$ unit cell in the y direction with respect to each other. The same shift of Ca,B- and Rh-layers for $\frac{1}{2}$ of unit cell along the z-direction was observed for $Ca_3Rh_8B_6$ structure but with a different sequence, and the only two of a total six Rh-layers contain two vacant cites each giving a $\frac{1}{9}$ missing atoms per unit cell, as compared to $CeCo_3B_2$.

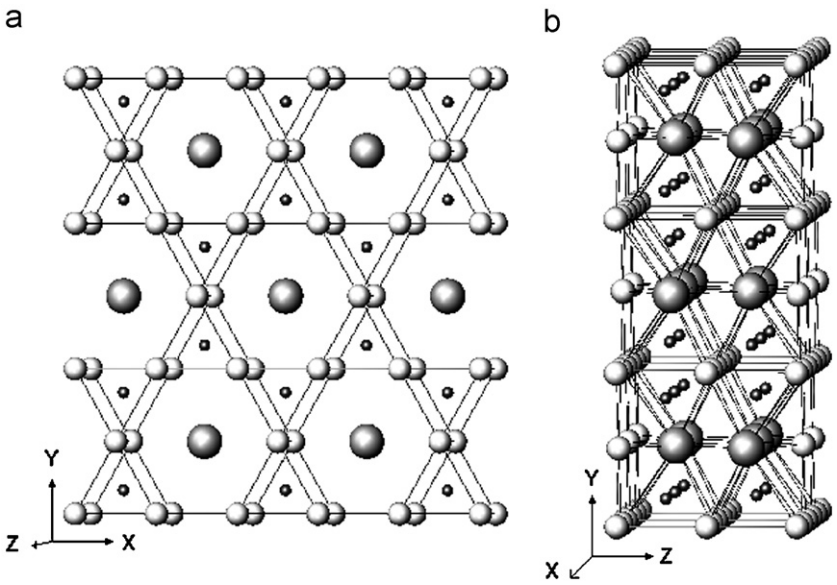

Fig. 6. B2 trigonal prisms layers (a) and B1 tetragonal antiprisms columns (b) in the structure of $La_3Ru_8B_6$.

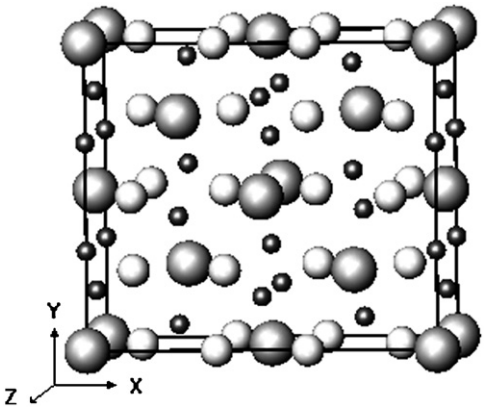

Fig. 7. The unit cell of $CaRh_2B_2$ structure. Large dark gray circles stand for calcium atoms, smaller light gray circles—for rhodium atoms, small black circles stand for B atoms.

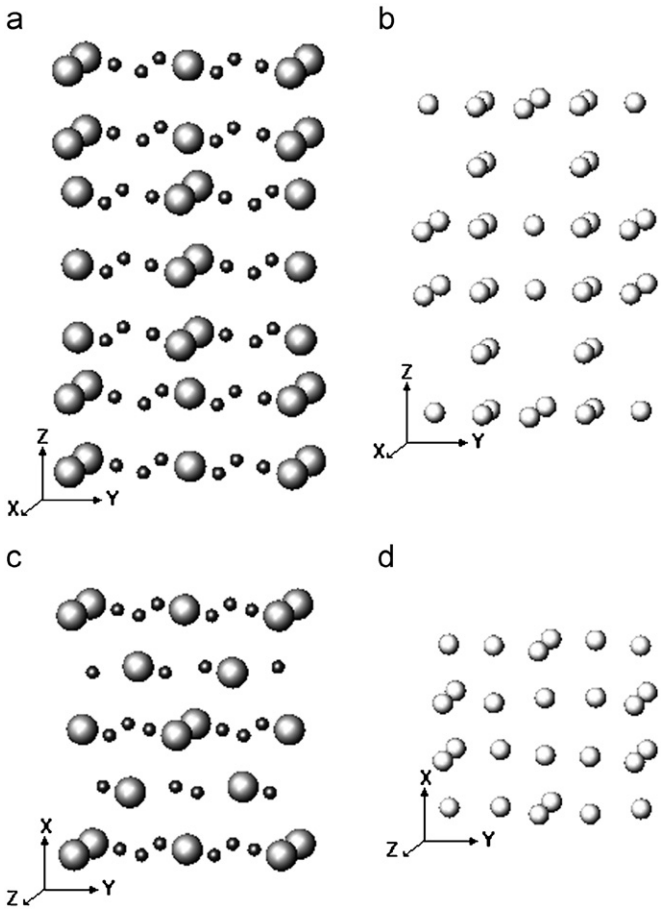

Fig. 8. Ca,B- and Rh-layers in the structures of $Ca_3Rh_8B_6$ (a, b) and $CaRh_2B_2$ (c, d). Large dark gray circles stand for calcium atoms, smaller light gray circles—for rhodium atoms, small black circles stand for B atoms.

Acknowledgments

The work of O.S. at the Institute of Nuclear Technology, Sacavém, Portugal was supported by the FCT grant (project SFRH/BPD/18810/2004). This work was partially supported by POCTI, under contract Nr. QUI/46066/2002.

References

[1] P. Rogl, in: K. Gschneidner, L. Eyring (Eds.), Handbook on the Physics and Chemistry of Rare Earths, vol. 6, Elsevier, Amsterdam, 1984 (Chapter 49).
[2] Yu.B. Kuz'ma, N.F. Chaban, Binary and Ternary Systems Containing Boron, Metallurgiya, Moscow, 1990.
[3] R.N. Shelton, B.A. Karcher, D.R. Powell, Mater. Res. Bull. 15 (10) (1980) 1445.
[4] R. Sobchak, P. Rogl, J. Solid State. Chem 27 (3) (1979) 343.
[5] H.C. Ku, Thesis, University of California at San Diego, USA, 1980.
[6] K. Hiebl, P. Rogl, H. Nowotny, J. Solid State. Chem. 54 (3) (1984) 414.
[7] O.L. Sologub, P. Salamakha, E.B. Lopes, H. Noël, A. Casaca, A.P. Gonçalves, in: Eighth Prague Colloquium on f-Electron Systems, Prague, Czech Republic, September 8–11, 2006, p. O-34.
[8] Yu.B. Kuz'ma, P.I. Krypyakevych, N.S. Bilonizko, Dopov. Akad. Nauk USSR A 10 (1969) 939.
[9] H.C. Ku, G.P. Meisner, J. Less-Common Met. 78 (1) (1981) 99.
[10] P. Salamakha, O. Sologub, Ch. Mazumdar, E. Alleno, H. Noel, M. Potel, C. Godart, J. Alloys Compds. 351 (2003) 190.
[11] A. Belger, G. Zahn, B. Wehner, P. Paufler, G. Graw, G. Behr, J. Alloys Compds. 283 (1999) 26.
[12] Yu.B. Kuz'ma, N.S. Bilonizhko, Kristallographiya 18 (4) (1973) 710.
[13] Yu.B. Kuz'ma, N.S. Bilonizhko, Dopov. Akad. Nauk USSR A 10 (1981) 87.
[14] Yu.B. Kuz'ma, O.M. Dub, N.F. Chaban, Dopov. Akad. Nauk USSR B 7 (1985) 36.
[15] Nonius, COLLECT: KappaCCD Software, Nonius BV, Delft, The Netherlands, 1998.
[16] T. Roisnel, J. Rodriguez-Carvajal, WinPLOTR: a Windows tool for powder diffraction patterns analysis, Materials Science Forum, in: R. Delhez, E.J. Mittenmeijer (Eds.), Proceedings of the Seventh European Powder Diffraction Conference (EPDIC 7), 2000, pp. 118–123.
[17] P.E. Werner, TREOR90, Program for Trail and Error Indexing of Powder Patterns, University of Stockholm, 1990.
[18] A. Boultif, D. Louer, Indexing of powder diffraction patterns for low-symmetry lattices by the successive dichotomy method, J. Appl. Crystallogr. 24 (1991) 987.
[19] G. Nolze, W. Kraus, PowderCell 2.1 Program, BAM, Berlin, 1999.
[20] J. Rodriguez-Carvajal, FullProf.2k, Laboratoire Leon Brillouin (CEA-CNRS), 2001.
[21] A.J.M. Duisenberg, L.M.J. Kroon-Batenburg, A.M.M. Schreurs, J. Appl. Crystallogr. 36 (2003) 220.
[22] G.M. Sheldrick, SADABS Version 2.03, Bruker AXS Inc., Madison, WI, USA, 2002.
[23] L.J. Farrugia, J. Appl. Crystallogr. 32 (1999) 837.
[24] T. Hahn (Ed.), International Tables for Crystallography, vol. A, Space Group Symmetry, D. Reidel, Dordrecht, 1983.
[25] G.M. Sheldrick, SHELXS-97, Program for the Solution of Crystal Structures, University of Göttingen, Germany, 1997.
[26] G.M. Sheldrick, SHELXL-97, Program for the Crystal Structure Refinement, University of Göttingen, Germany, 1997.
[27] E. Parthé, K. Cenzual, R. Gladyshevskii, J. Alloys Compds. 197 (1993) 291.
[28] G. Caglioti, A. Paoletti, F.P. Ricci, Nucl. Instrum. 3 (1958) 223.
[29] Yu.B. Kuzma, Crystal Chemistry of Borides, Lviv, Vyshcha Shkola, 1983.
[30] P. Rogl, Monatsh. Chem. 104 (1973) 1623.
[31] O.S. Zarechnyuk, P.I. Krypyakevych, E.I. Gladyshevskii, Sov. Phys. Crystallogr. 9 (1964) 706.
[32] P.I. Krypyakevych, Structure types of Intermetallic Compounds, Moskva, Nauka, 1977.
[33] W. Jung, J. Less-Common Met. 97 (1984) 253.
[34] B. Schmidt, W. Jung, Z. Naturforsch. 33b (1978) 1430.
[35] C. Horwath, P. Rogl, K. Hiebl, J. Solid State Chem. 67 (1987) 70.